Food Hydrocolloids 51 (2015) 281–294

Contents lists available at ScienceDirect

Food Hydrocolloids

journal homepage: www.elsevier.com/locate/foodhyd

Chitosan molecular weight effect on starch-composite film properties

María Julieta Bof [a], Valeria Carina Bordagaray [a], Delia Elisa Locaso [a], María Alejandra García [b, *]

[a] Facultad de Ciencias de la Alimentación, Universidad Nacional de Entre Ríos, Monseñor Tavella 1450, Concordia, 3200, Entre Ríos, Argentina
[b] CIDCA (Centro de Investigación y Desarrollo en Criotecnología de Alimentos), Facultad Ciencias Exactas Universidad Nacional de La Plata (UNLP) – CONICET La Plata, 47 y 116 S/N°, La Plata, B1900AJJ, Buenos Aires, Argentina

ARTICLE INFO

Article history:
Received 17 March 2015
Received in revised form
23 April 2015
Accepted 4 May 2015
Available online 30 May 2015

Keywords:
Chitosan molecular weight
Starch
Mechanical properties
Water vapor permeability
Physico-chemical properties
Microstructural analysis

ABSTRACT

The aim of this work was to prepare and characterize composite films based on chitosan (CH) and corn starch (CS), analyzing the influence of the chitosan molecular weight (MW) on film structure and functional properties. Three chitosan products were characterized and classified as low (LMW), medium (MMW) and high (HMW) according to its MW. Rheological behavior of filmogenic solutions depend on CH-MW from Newtonian to pseudoplastic one. Chitosan based film physicochemical properties were strongly affected by its molecular weight: the lower the MW the higher the color differences and film solubility. SEM observations demonstrated that plasticized chitosan films exhibited homogeneous structures, the higher the MW the more compact is the structure and the lower is the water vapor permeability (WVP, $4.55 \pm 0.6 \times 10^{-11}$ g/m s Pa.). Likewise, CH and CS were compatible polymers which led to the development of homogeneous blend films. Polymer interactions were evidenced in FTIR spectra by the shifts observed within the region of 1500–1700 cm^{-1}, which reduce the hydrophilic groups' availability of chitosan matrices, leading to a reduction in WVP of composite films. Mechanical properties of the developed films were performed through different complementary tests. Chitosan MW affects both the type and number of interactions, which determine the matrix structure and characteristics. In HMW-CH matrix polymer–polymer interactions are favored, leading to strong and resistant matrices with high dynamic elastic modulus values. Meanwhile, in LMW-CH one, polymer-plasticizer and polymer–solvent interactions became important and the development of high extensible and soluble materials is privileged.

1. Introduction

The use of industrial by-products as well as polymers derived from biomass is attracting increasing interest both in academia and in the potential commercial applications. Within this context, this paper will focus on the use of polysaccharides for biodegradable composite films formulation. These materials derived from renewable sources, exhibited a significative higher degradation rate than petroleum-derived plastic one and also contribute to extend the food shelf-life (Xu, Kim, Hanna, & Nag, 2005).

Among natural biopolymers available to produce biodegradable films, starch is one of the most commonly used materials due to its availability, low cost, biodegradability and renewability (Avérous, Fringant, & Moro, 2001). However, its applications are limited due to its high water affinity and brittleness (Mathew Brahmakumar & Abraham, 2006; Wu & Zhang, 2001). To improve these drawbacks and provide further functional properties, usually starch is combined with other natural biopolymers to form composite films. Due to its film forming property, excellent biocompatibility and antimicrobial activity, chitosan is widely used for this purpose (Dutta, Tripathi, Mehrotra, & Dutta, 2009; Park, Marsh, & Rhim, 2002; Pelissari, Grossmann, Yamashita, & Pineda, 2009; Sánchez-González, Cháfer, Chiralt, & González-Martínez, 2010).

Chitosan is a copolymer of D-glucosamine and N-acetyl-Dglucosamine obtained from chitin. The term chitosan usually refers to a family of chitin derivatives obtained after partial deacetylation to not only varying degrees but also different molecular weights. When the average degree of acetylation becomes lower than 50 mol%, the product turns soluble in acidic conditions due to the protonation of the NH_2 group at the C-2 position of glucosamine units (Rinaudo, 2006; Younes, Sellimi, Marguerite Rinaudo, Jellouli,

* Corresponding author. Tel./fax: +54 221 4254853.
E-mail address: magarcia@quimica.unlp.edu.ar (M.A. García).

http://dx.doi.org/10.1016/j.foodhyd.2015.05.018
0268-005X/

& Nasri, 2014). As it is well known, chitosan is the unique existing natural positively charged polysaccharide.

The chitosan production process involves an acid treatment (decalcification), an alkaline treatment (deproteinization) and a decolorization step. Subsequently, a new alkali treatment is applied to produce the deacetylation of chitin. In this process, there are multiple factors that can vary the properties of chitosan obtained, such as the alkali concentration, incubation time, chitin-alkali ratio, temperature, atmosphere, chitin source (including the polymorphism), particle size, heterogeneous/homogeneous N-deacetylation and single or multiple process (Van den Broek, Knoop, Kappen, & Boeriu, 2015). Commercial chitosan usually has a deacetylation degree (DD) ranging from 70 to 95% and a molecular weight within the range of 10^4–10^6gmol^{-1} (Motta de Moura, Motta de Moura, Madeira Soares, & de Almeida Pinto, 2011). Thus, available products present a wide range of characteristics, which define its applications and influence the final performance of the biopolymer. Recent studies have revealed that the antimicrobial effect of chitosan is related to chitosan characteristics: molecular weight and acetylation degree (Arancibia et al., 2015; Chen & Zhao, 2012). Antibacterial activity of chitosan against Gram-negative bacteria increases with decreasing acetylation degree, MW and pH (Younes et al., 2014).

The reasons for chitosan addition in composite formulations are the good film forming and mechanical properties, no toxicity, biodegradability, relative hydrophobic polymer nature that could provide higher moisture barrier and water resistance (Bangyekan, Aht-Ong, & Srikulkit, 2006; Mathew & Abraham, 2008).

The aim of this work was to prepare and characterize composite films based on chitosan and corn starch, analyzing the influence of the chitosan molecular weight on film structure and functional properties such as mechanical and barrier properties, which are relevant for food packaging applications.

2. Materials and methods

2.1. Materials

Three chitosan products (CAS 9012-76-4) having different molecular weights (MW) were used: a 2.5% (w/w) commercial solution RaiSan® (Ftalosur SA, Buenos Aires, Argentine; supplier reference number: 6A/F47/5000/1.5.13) with low molecular weight (LMW), a chitosan powder (Parafarm, Buenos Aires, Argentine; supplier reference number: 11017A) with medium molecular weight (MMW) and a chitosan powder (Sigma, St. Louis, MO, USA; supplier reference number: 48165) with high molecular (HMW), being the last one derived from crab shells. All of them had a deacetylation degree of 85%, informed by the suppliers.

Corn starch was purchased from Glutal (Buenos Aires, Argentine; food grade) containing 25% amylose. This polysaccharide presents an average molecular weight of 2×10^4 g mol^{-1} for amylose and 2×10^5–1×10^6 g mol^{-1} for amylopectin. Glycerol (Anedra, Buenos Aires, Argentine) was used as plasticizer in all formulations.

2.2. Chitosan viscosity average molar weight

Chitosan diluted solutions (0.001–0.005 g mL^{-1}) were prepared using an aqueous system composed of acetic acid (Anedra, Buenos Aires, Argentine) 0.1 M and sodium chloride (Anedra, Buenos Aires, Argentine) 0.2 M as solvent. Solutions were filtered before the viscosity determinations, which were carried out at the lowest shear velocities permitted within the experimental error and the Newtonian plateau, which is a requirement for this method (Ravi Kumar, 2000). Relative viscosity was then measured with a Cannon-Fenske (200 series, model 120205, IVA, Argentine) capillary viscometer at 25.0 ± 0.1 °C. Draining time of a fixed volume of the diluted solutions of chitosan (t) and solvent (t_0) content between two consecutive marks of the capillary was measured. From these, specific viscosity (η_{sp}) and relative viscosity (η_r) were calculated according to the following equations:

$$\eta_r = \frac{\eta}{\eta_0} \approx \frac{t}{t_o} \tag{1}$$

$$\eta_{sp} = \frac{(\eta - \eta_o)}{\eta_0} \approx \frac{(t - t_0)}{t_o} \tag{2}$$

where η and η_0 are the solution and solvent viscosities, respectively.

The relationship between the viscosity and the concentration was empirically demonstrated by Huggins (1942) and Kramer (1938), which can be described by the following equations:

$$\frac{\eta_{sp}}{c} \approx [\eta] + k_H[\eta]^2 c \tag{3}$$

$$\frac{\ln \eta_r}{c} \approx [\eta] + k_K[\eta]^2 c \tag{4}$$

where k_H and k_K are the Huggins and Kramer constants (dimensionless), respectively and c is the concentration of the solution, in g mL^{-1}. For dilute solutions, two straight lines are obtained, which extrapolated to zero concentration, agree on the intrinsic viscosity [η]. This parameter, expressed in mL g^{-1}, is a measure of the hydrodynamic volume that the macromolecules occupied in solution, it is associated to polymer size and it allows estimating the molecular weight of the polymer in solution. Thus, the viscosity average molecular weight (M_η) of chitosan was calculated from the experimental intrinsic viscosity [η] data using the Mark-Houwink-Sakurada-Staudinger equation.

$$[\eta] = K \times (M_\eta)^a \tag{5}$$

where K = 1.81 10^{-3} mL/g and a = 0.93 (Roberts & Domszy, 1982).

2.3. Chitosan deacetylation degree

The degree of deacetylation is determined by potentiometric titration according to method described by Motta de Moura et al. (2011) with slight modifications. 0.3 g chitosan were weighed and dissolved in 25 mL of 0.1 M HCl (Anedra, Buenos Aires, Argentine) solution. The ionic strength was adjusted to 0.1 M by adding KCl (Anedra, Buenos Aires, Argentine) to the solution. Potentiometric titration was performed with standard NaOH (Anedra, Buenos Aires, Argentine) 0.1 M solution using an EC30 HACH pH-meter (HACH Instruments, Loveland, CO, USA). The end point of the titration was determined by the first derivative method from the obtained titration curve (pH vs. titrant volume). Deacetylation degree (DD) was calculated as the percentage of free amino groups present in the sample, according to the following equation:

$$DD\ (\%) \equiv NH_2(\%) = \frac{16.1 \times (V_{e2} - V_{e1}) \times C_{NaOH}}{weight\ sample} \tag{6}$$

Where V_{e2} and V_{e1} are the volume of the second and first equivalence point, respectively and C_{NaOH} is the concentration of the titrant used. Determinations were carried out at least by triplicate.

2.4. Film forming suspension/solution preparation

A 4% (w/w) corn starch suspension (CS) was prepared, which was gelatinized for 20 min at 85 °C. Furthermore, MMW and HMW chitosan (CH) powder were dissolved in acetic acid 1.25% (w/w) in order to obtain 2.5% (w/w) chitosan solutions, under stirring for 24 h. LMW chitosan solution was directly used.

One-component suspensions/solutions were analyzed (100% CS or 100% CH) as well as a blend of them (50CS:50CH), obtained by mixing the individual suspensions in equal weight proportions. Blend proportion was selected from preliminary tests (Bof, García, Locaso, & Zambón, 2014).

In all formulations glycerol as plasticizer was added to 25% w/w solids; this concentration was selected from preliminary performed tests. Likewise, the filmogenic suspension homogenization was carried out with a digital homogenizer (Ultra Turrax, IKA T-25, Germany) for 1.5 min at 24000 rpm. Subsequently, the mixtures were treated with a vacuum pump for 15 min to ensure air bubbles removal which could affect the obtained film properties.

2.5. Filmogenic suspension rheological characterization

Rheological assays of film forming suspensions were performed in a Rheo Stress 600 ThermoHaake (Haake, Germany) rheometer using a plate–plate system PP35 (1 mm gap) at controlled temperature (20 °C). Rotational mode was used to investigate time-dependent behavior of filmogenic suspensions as described in a previous work (López, García, & Zaritzky, 2008). The resulting curves were mathematically modeled as Ostwald de Waele fluids by the following equation:

$$\tau = k \times \dot{\gamma}^{n} \tag{7}$$

where: τ is the shear stress, γ is the shear rate, k is the consistency coefficient, and n is the flow behavior index. The apparent viscosity of filmogenic suspensions was determined at 500 s^{-1}. Rheological tests were performed at least in triplicate for each formulation.

2.6. Film preparation

Films were prepared by casting 20 g filmogenic suspensions onto Petri dishes (9 cm diameter) and dried at 50 °C in an oven until reaching constant weight. The obtained films were removed from the dishes and conditioned (4 days at 60% relative humidity and 25 °C) prior to the determinations of the physicochemical, barrier and mechanical properties.

2.7. Film properties

Film color was measured using a colorimeter (CR-300 Minolta, Japan), previously calibrated with a white plate (Y = 93.2, x = 0.3133 and y = 0.3192). The CIELAB color scale was used, where L^* is the luminosity, a^* is the greenness and redness of samples and b^* represents the blueness and yellowness. Film specimens were placed on the white plate, and at least five measurements were taken from the sample surfaces.

Total color differences (ΔE) were calculated as:

$$\Delta E = \sqrt{\left((a^* - a_0^*)^2 + \left(b^* - b_0^*\right)^2 + \left(L^* - L_0^*\right)^2\right)} \tag{8}$$

where: a_0^*, b_0^* and L_0^* are the standard parameters and a^*, b^* and L^* are the sample parameters.

Humidity content was determined by measuring the weight loss of films, upon drying in an oven at 105 °C until constant weight. Samples were analyzed in duplicate.

Film solubility in water at 25 °C was determined according to the method described by López et al. (2008) on film pieces of 4 cm^2 in 80 mL distilled water under 200 rpm agitation during 1 h. The reported results corresponded to the mean of two replicate assays.

Water vapor permeability (WVP) tests were conducted using ASTM method E96 (ASTM, 2012) with several modifications. After steady-state condition was reached, the aluminum permeation cells (Payme Elcometer 5100, Manchester, UK) were weighed (0.0001 g) at initial time and at 1 h interval for 8 h. A constant gradient of water vapor partial pressure across the samples used was 2000 Pa, since measurements were performed at 5 °C. The changes in cell weight were determined through time in an analytical scale. The results were lineally regressed and the slope allowed calculating the water vapor transmission rate (WVTR, in g s^{-1} m^{-2}) and considering the film tested thickness the WVP (g/m s Pa) was calculated. The informed values are the mean of at least two determinations.

Film thickness was determined by using a digital coating thickness gauge Check Line DCN-900 (New York, USA) for non-conductive materials on non-ferrous substrates. At least ten measurements were taken from each sample.

Dynamic mechanical analyses (DMA) were conducted in a Q800 (TA Instruments, New Castle, USA) equipment with a liquid N_2 cooling system, using a clamp tension and rectangular film probes (length: 30 mm, width: 6 mm and thickness: determined as described previously). To select the viscoelasticity range for further frequency sweeps, amplitude sweep were performed from 1 to 20 μm at fixed frequency (5 Hz). Multi-frequency sweeps (3–20 Hz) at fixed amplitude (5 μm) from −100 to 150 °C at 5 °C min^{-1} were carried out, with an isotherm of 5 min at −100 °C. Storage (E′), loss (E″) modulus, and tan δ (E″/E′) curves as a function of temperature were recorded and analyzed using the software Universal Analysis 2000 (TA Instruments, New Castle, USA). Temperatures of the relaxation processes associated with glass transition temperatures were determined through the inflection point of the storage modulus E′ curve as well as the maximum peak in both the loss modulus E″ and tan δ curves.

For quasi-static test in uniaxial condition, a constant force ramp rate of 0.3 N/min was applied to record the stress–strain curves until rupture from film sample strips or up to 18 N, using the same DMA as in the case of dynamic tests. Tests were carried out at 25 °C. The dynamic elastic modulus (E_c, MPa) of film samples were determined by mathematical modeling of stress-strain curves obtained by DMA, in accordance with model used by Chillo et al. (2008), (eq. (9)):

$$\sigma_\tau = E_c \times \varepsilon_\tau \times e^{(-\varepsilon_\tau \times K)} \tag{9}$$

where σ_τ and ε_τ are the true strain and the true stress, respectively, calculated according to Mancini, Moresi, and Rancini (1999); and K is a constant value, regarded as a fitting parameter. Informed results correspond to the mean of at least five determinations.

Mechanical profiles (stress-strain curves) were obtained using a texturometer TA.XT2i-Stable Micro Systems (England) with a tension grip system A/TG. Probes of 6 cm in length and 0.7 cm in width were cut from conditioned films. At least ten probes were tested for each film formulation. Tensile strength (TS, MPa), elasticity modulus (Young's modulus, MPa) and elongation at break (EB, %) were calculated as described by López, Lecot, Zaritzky, and García (2011).

Puncture tests were also performed in the mentioned texturometer using a cylindrical probe 2 mm in diameter (P/2). The force vs. deformation curves were recorded and the maximum force (N)

and deformation (mm) of each conditioned film were determined, as well as the area under the curve (N mm) in puncture test. This parameter is indicative of the amount of energy that a film absorbs before puncture.

2.8. Microstructural analyses

Scanning electron microscopy (SEM) analyses were carried out using a JEOL JSM-6300 (Japan) microscope. Samples were maintained in a desiccator with P_2O_5 for two weeks prior to SEM analysis; films were cryofractured by immersion in liquid nitrogen for cross-section observations. Then, film pieces were mounted on copper stubs, coated with a gold layer and observed using an accelerating voltage of 10 kV, under high vacuum mode.

Fourier transformed infrared (FTIR) spectra of the films were carried out on an IR spectrophotometer ((Nicolet, iS10 Thermo Scientific, Madison, USA). Spectra were recorded between 4000 and 400 cm^{-1} by accumulation of 64 scans at 4 m^{-1} resolution. Data were analyzed by using the software Omnic 8 (Thermo Scientific, Madison, USA).

2.9. Statistical analysis

For the statistical analysis of the results, the Statgraphics Centurion XV Software (Statgraphics Co., Tulsa, OK, USA) was used. Analysis of variance (ANOVA) and comparison of means with the Fisher's least significant difference (LSD) test were conducted, at a significance level $p = 0.05$.

3. Results and discussion

3.1. Chitosan molecular characteristics

It was not possible to estimate the molecular weight and degree of acetylation of chitosan dissolved in the commercial solution, so the features provided by the supplier are reported. Table 1 shows the molecular characteristics of different used chitosans, non significant ($p > 0.05$) differences in the degree of acetylation were detected. The significantly different viscosity average molecular weights (M_η) of the chitosans indicate that the used polymers exhibited different polymerization degrees. Thus, chitosan used in this work was classified according to its molecular weight and the effect of this characteristic on film-forming rheological behavior and film properties was studied.

Chitosan is produced mainly from the exoskeletons of crustaceans, basically by four steps: demineralization, deproteinization, decolourization and deacetylation. Chitosan extraction procedure modifications yielded chitosans with different molecular weights and DD. Arancibia et al., (2015) stressed that DD was only slightly affected by the different processing conditions, but M_η was affected much more. Thus, these authors informed for chitosan with 84% DD M_η varying from 690 to 5600 kDa. Likewise, Beaney, Lizardi-Mendoza, and Healy (2005) and Sini, Santhosh, and Mathew (2007) obtained low molecular weight chitosan (70.3 and 256 kDa, respectively) from chitin extracted by lactic fermentation of shellfish waste, pointing out the effect of material raw. In this sense, Martinez-Camacho et al. (2010) indicates that the obtention of low molecular weight chitosan could be attributed to greater susceptibility to degradation of chitin and/or depolymerization during the removal of proteins and minerals, and in the purification procedures and subsequent deacetylation.

Table 1
Rheological parameters of plasticized filmogenic suspension formulated with corn starch, different molecular weight chitosan and the blend of both in equal proportions.

Chitosan	*Viscometric molecular weight determination*				*Deacetylation degree (%)*
	Intrinsic viscosity [η] (mL/g)			Viscosity average molecular weight (M_η, kDa)	
	[η] estimated by Equation 3	[η] estimated by Equation 4	Average [η] used in Equation 5		
LMW	–	–	–	270[a*]	85[a*]
MMW	325.53[a]	320.95[a]	323.24[a]	444[b]	83.72 ± 3.22[a]
HMW	929.42[b]	938.83[b]	934.12[b]	1390[c]	86.25 ± 0.47[a]

*Informed by the supplier. LMW: low molecular weight, MMW: medium molecular weight and HMW: high molecular weight chitosan. Reported values correspond to the mean ± standard deviation. Different letters in the same column indicate significant differences ($p < 0.05$).

3.2. Filmogenic suspension rheological characterization

The study of filmogenic suspension rheological behavior allows determining their processing conditions. It is important to notice that polymer concentration in the film-forming formulation is critical, since high polymer concentrations led to high viscosity solution which are difficult to dissolving, handling and transport. By contrast, excessively low viscosity and dilute solutions result in problems associated with the inability to form films or coatings that may adhere to a specific product/support. Also, film thickness is determined by the filmogenic suspension viscosity as well as the molding ratio (weight of filmogenic suspension to plate area) when they are obtained by casting technique. Rheological characteristics also condition the structural properties of drying materials such as density, presence of pores and cracks associated with the difficult elimination of bubbles from highly viscous solutions (Han & Gennadios, 2005). The development of a dense matrix without defects is necessary to obtain materials with suitable mechanical and barrier properties.

Rotational assays led to analyze filmogenic suspensions' rheological behavior when they are submitted under conditions close to industrial processing parameters such as high shear stress. Corn starch filmogenic suspension exhibited a pseudoplastic behavior ($n < 1$), which was satisfactorily adjusted by the Ostwald de Waele model (Table 2). Chitosan filmogenic solutions rheological behavior depended on chitosan molecular weight. While LMW chitosan solution presented a practically Newtonian behavior ($n = 0.96$), MMW and HMW chitosan solutions resulted pseudoplastics, increasing both consistency index and apparent viscosity, and consequently decreasing the flow behavior index, with polymer molecular weight (Table 2). Apparent viscosity of CH solutions was higher than that of corn starch suspensions, being 2.4, 5.3 and 7.8 times higher for LMW, MMW and HMW, respectively. These results evidenced that macromolecules' structural aspects such as molecular weight (between others like polymerization degree and chains size distribution) determine the developed network characteristics. Casettari, Cespi, Palmieri & Bonacucina (2013) stressed that different molecular mechanisms (e.g. hydrogen bonding, electrostatic and hydrophobic interactions) are involved in the rheological behavior of chitosan systems.

The blend suspensions formulated with LMW chitosan exhibited a similar Newtonian behavior, while MMW and HMW blends remained pseudoplastics. In general, intermediate consistency index and apparent viscosity were obtained for blend suspensions compared to individual component ones.

Table 2 shows that in general consistency index and apparent viscosity of the filmogenic suspensions analyzed follow a similar trend.

Table 2
Rheological parameters of plasticized filmogenic suspension formulated with corn starch, different molecular weight chitosan and the blend of both in equal proportions.

Filmogenic suspension	Chitosan molecular weight (MW)	Ostwald de Waele mathematical model			Apparent viscosity at 500 s^{-1} (mPa s)
		r^2	Consistency index k (Pa s^{-n})	Flow behavior index n (s^n)	
Corn starch (CS)*	–	0.9783	0.365 ± 0.007^{e}	0.63 ± 0.04^{a}	32.89 ± 2.4^{a}
50 CS: 50 CH	LMW	0.9999	0.07 ± 0.001^{a}	0.96 ± 0.003^{e}	55.30 ± 2.05^{b}
	MWM	0.9998	0.34 ± 0.01^{d}	0.82 ± 0.00^{d}	110.06 ± 0.56^{d}
	HMW	0.9995	0.265 ± 0.03^{c}	0.682 ± 0.004^{b}	128.32 ± 0.45^{e}
Chitosan (CH)	LMW	0.9999	0.10 ± 0.003^{b}	0.96 ± 0.005^{e}	80.52 ± 0.05^{c}
	MWM	0.9997	0.62 ± 0.04^{f}	0.80 ± 0.01^{c}	174.46 ± 2.80^{f}
	HMW	0.9990	3.19 ± 0.08^{g}	0.605 ± 0.005^{a}	255.57 ± 11.12^{g}

*CS: 4% (w/w) corn starch gelatinized suspension, CH: 2.5% (w/w) CH solution and 50CS: 50CH: the blend of them in equal proportion (w/w). All formulations contain glycerol as plasticizer to 25% w/w solids. LMW: low molecular weight, MMW: medium molecular weight and HMW: high molecular weight chitosan. Reported values correspond to the mean ± standard deviation. Different letters in the same column indicate significant differences ($p < 0.05$).

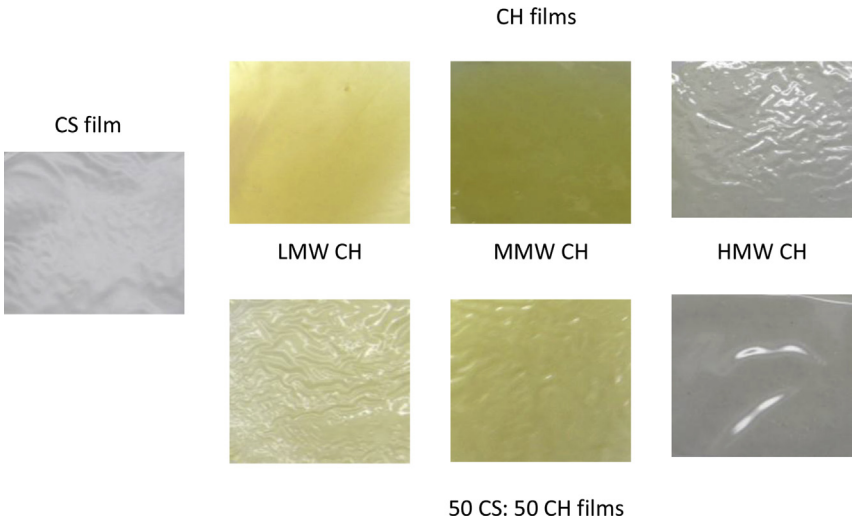

Fig. 1. Digital photographs of films based on corn starch (CS), chitosan (CH) and a blend of them in equal proportions (50CS: 50CH). LMW, MMW and HMW correspond to low, medium and high molecular weight chitosan.

3.3. Film appearance and color

All filmogenic suspension was able to form homogeneous films which were easily removed from the acrylic plates. It is worth noting that the films prepared with LMW and MMW chitosan had a slightly yellowish color (Fig. 1). Film thickness is presented in Table 3; in CH films the molecular weight of the chitosan used did not affect film thickness. For blend films the higher the molecular weight the higher the thickness, although differences were significative ($p < 0.05$) only in the case of LMW and HMW-CH based films. Corn starch films exhibited thickness values around 80 μm. Film thickness comparison with those reported for hydrocolloid-based films is difficult because casting ratio used is generally omitted.

Fig. 2 shows film color results for CS and CH films as well as the blend. Luminosity of CS films exhibited higher values than CH films while blend films presented intermediate values, regardless the MW of the chitosan used. Although, luminosity differences were marked for films formulated with low MW (Fig. 2a).

Table 3
Puncture mechanical parameters, thickness and humidity content of plasticized films formulated with corn starch, different molecular weight chitosan and the blend of both in equal proportions.

Film formulation	Chitosan molecular weight (MW)	Puncture mechanical parameters			Film thickness (μm)	Humidity content (%)
		Maximum force (N)	Deformation (mm)	Area under the curve (N mm)		
Corn starch (CS)*	–	5.53 ± 0.32^{e}	1.81 ± 0.07^{a}	5.32 ± 0.06^{a}	80.72 ± 2.15^{b}	14.60 ± 0.73^{a}
50 CS: 50 CH	LMW	10.81 ± 1.08^{b,c}	2.17 ± 0.29^{b}	12.65 ± 2.05^{d}	66.17 ± 2.76^{a}	21.81 ± 0.15^{b}
	MWM	2.70 ± 0.46^{a}	2.92 ± 0.23^{c}	7.18 ± 1.12^{b}	72.94 ± 7.27^{a,b}	26.75 ± 0.73^{c}
	HMW	17.23 ± 1.06^{d}	3.28 ± 0.42^{c,d}	28.25 ± 2.21^{f}	82.00 ± 2.98^{b,c}	13.95 ± 0.51^{a}
Chitosan (CH)	LMW	9.65 ± 1.24^{b,c}	3.66 ± 0.17^{d}	17.38 ± 2.89^{e}	77.72 ± 6.67^{b}	31.60 ± 0.88^{d}
	MWM	8.87 ± 0.83^{b}	3.63 ± 0.42^{d}	16.80 ± 4.18^{d,e}	86.22 ± 2.34^{b,c}	23.41 ± 1.12^{b,c}
	HMW	10.23 ± 2.66^{b,c}	1.82 ± 0.24^{a}	9.31 ± 0.62^{c}	88.38 ± 7.86^{b,c}	14.97 ± 0.86^{a}

*CS: 4% (w/w) corn starch gelatinized suspension, CH: 2.5% (w/w) CH solution and 50CS: 50CH: the blend of them in equal proportion (w/w). All formulations contain glycerol as plasticizer to 25% w/w solids. LMW: low molecular weight, MMW: medium molecular weight and HMW: high molecular weight chitosan. Reported values correspond to the mean ± standard deviation. Different letters in the same column indicate significant differences ($p < 0.05$).

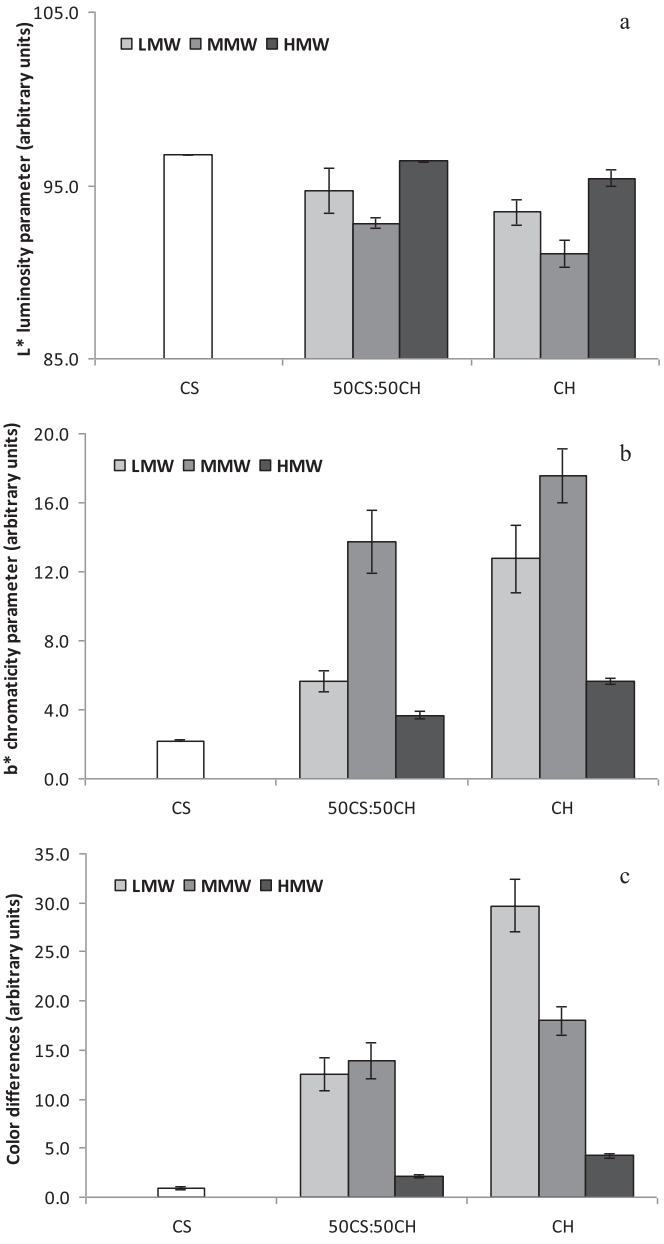

Fig. 2. Color parameters of films based on corn starch (CS), chitosan (CH) and a blend of them in equal proportions (50CS: 50CH): a) luminosity parameter, b) b* chromaticity parameter and c) color differences. LMW, MMW and HMW correspond to low, medium and high molecular weight chitosan.

Chitosan film luminosity depended on the molecular weight of the biopolymer used, although higher values were found for LMW followed by MMW, a clear trend could not be established. These observed differences could be attributed to the chitosan source, which in the case of LMW and MMW chitosan were unreported. Several authors have stressed the chitosan source effect on their properties and specifically their color attributes (Hwang, Kim, Jung, Cho, & Park, 2003).

The chromaticity parameter b* exhibited the most important changes (Fig. 2b). In all cases, b* values of CS films were lower than those of CH ones, presenting the blends intermediate but significantly ($p < 0.05$) different values than those of one component films. In general, films based on polysaccharides are typically colorless, although those of CH were slightly yellowing, which has been attributed to Maillard reactions between amino and hydroxyl groups of chitosan molecules (López et al., 2014). Likewise, CH based film b* values depend on the molecular weight of the polymer, showing LMW chitosan based films lower values than those of MMW ones, although, again, a clear tendency could not be established, probably due to chitosan source differences.

Film color differences follow a similar trend than b* chromaticity parameter. In general CS films presented lower ΔE values than the blend films, being both lower than CH-based films, regardless of MW (Fig. 2c). However, analyzing the values obtained for CH films a clear tendency could be found with molecular weight, the lower the MW the higher the ΔE. In this case the effect of both luminosity and b* parameter were potentiated. HMW-chitosan based films led to the lower ΔE color differences, which is of primary importance since regarding packaged goods the visual properties of the films determine the overall acceptability of consumers.

3.4. Water vapor barrier properties and film solubility

CS films exhibited a value ($1.96 \pm 0.27 \times 10^{-10}$ g/m s Pa) within the range of those reported for other corn starch films (García, Famá, Dufresne, Aranguren, & Goyanes, 2009; López et al., 2008). Water vapor barrier properties of CH films depend on the molecular weight of the polymer used, the obtained WVP values were: $4.14 \pm 0.26 \times 10^{-10}$ g/m s Pa for LMW, $3.38 \pm 0.11 \times 10^{-10}$ g/m s Pa for MMW while HMW chitosan films presented a value of $4.55 \pm 0.6 \times 10^{-11}$ g/m s Pa. In this sense, it is important to note that WVP of LMW chitosan films was 9 times higher than those of HMW ones. These results indicate that the higher the chitosan MW the lower the film WVP, being differences statistically significant ($p < 0.05$), (Fig. 3a), probably due to the development of a more compact structure by higher polymerization degree chitosan chains. Leceta, Guerrero, and de la Caba (2013) found a similar trend working on films formulated with two different molecular weight chitosans, although the authors did not specify them and the DD of the polymer was 75%.

Motta de Moura et al. (2011) have stressed that molecular weight and deacetylation degree changes would provide changes in biofilm hydrophilicity and cristallinity, and consequently, changes in water vapor permeability and mechanical properties of the biofilm obtained from chitosan. Likewise, a lower interaction degree between glycerol and chitosan was observed in the case of LMW chitosan, which facilitates the water vapor molecules migration through the film (Leceta et al., 2013).

WVP values of HMW chitosan blend films did not statistically differ ($p > 0.05$) than that of the corresponding pure chitosan film. MMW and LMW chitosan blend films exhibited similar WVP values, which were intermediate between the individual component films, indicating the beneficial effect of corn starch addition on film barrier properties (Fig. 3a). The developed interactions between chitosan and corn starch, mainly hydrogen bonding type, reduces the hydrophilic groups availability of chitosan matrices, leading to a reduction in water vapor transmission rate. A similar explanation was argued by Chillo et al. (2008) in the case of chitosan films blended with tapioca starch.

Concerning to film water solubility, chitosan molecular weight drastically affected this physicochemical property, the lower the chitosan molecular weight the higher the solubility of the film (Fig. 3b). A similar trend was also reported by Leceta et al. (2013). Likewise, chitosan film solubility also depends on the deacetylation degree, the distribution of acetyl groups along the main chain and the nature of the acid used for protonation in the dissolving step (Pillai, Paul, & Sharma, 2009).

On the other hand, corn starch films exhibited a solubility value similar to that of the MMW chitosan one. In the case of blend films, those formulated with LMW or HMW chitosan presented solubility

values intermediate than the individual component films. Meanwhile for blend films formulated with MMW chitosan a synergic effect between both polymers was observed, recording a significantly ($p < 0.05$) lower value (Fig. 3b).

3.5. Dynamic mechanical analysis

In general, the linear viscoelastic range was around 12 μm for films containing starch and 15 μm for CH films, regardless the molecular weight of the chitosan. Thus, frequency sweep assays as a function of temperature was performed at constant amplitude of 5 μm.

Chitosan films exhibited, two relaxations, β and α, with increasing temperature, (Fig. 4a). The location of both transitions depended on the molecular weight of the chitosan used. For example, the β relaxation was located around −25.5, −14.5 and −19.6 °C for low, medium and high molecular weight respectively. Neto et al. (2005) and Mucha and Pawlak (2005) reported that chitosan films exhibited an event associated with β relaxation at around −20 to −10 °C, characteristic of the local motion of side groups in chitosan polysaccharide. The second peak in tan δ curves of dynamic mechanical spectra of CH films corresponded to α relaxation; the temperature at which it took place can be labeled as the dynamic glass transition temperature Tg, despite the frequency tested, and in this case it was found at 32.2, 46.8 and 81.4 °C for LWM, MMW and HMW CH films, respectively (Fig. 4a).

Plasticized corn starch film dynamic-mechanical patterns show two relaxations, one located at −41.6 °C, associated to the glass transition of the plasticizer-rich phase, and other at 57.8 °C, attributed to the starch-rich phase (Fig. 4b). Several authors stressed that starch-glycerol mixtures are partially miscible systems, given rise to starch-rich phase and other rich in glycerol (DaRoz, Carvalho, Gandini, & Curvelo, 2006; García et al., 2009; Mathew & Dufresne, 2002). Our results are in agreement with those reported by López et al. (2011) working on native and acetylated corn starch films. A similar trend was also reported by other authors for films formulated with native starches from different sources such as waxy maize (García et al., 2009), pea (Ma, Chang, Yu, & Stumborg, 2009) and cassava (Famá, Flores, Gerschenson, & Goyanes, 2006).

In the case of blend films, CH molecular weight did not affect the location of both peaks observed (Fig. 4b). While the peak of the first peak was located around −25 °C, closer to the values corresponding to the β transition in CH films, the second one was placed around 60 °C, closer to the values associated to the starch rich phase transition in CS films.

3.6. Film mechanical properties

A comprehensive study of the mechanical properties of the developed films was performed through different complementary tests. With regard to tensile assays, in general, plasticized developed films exhibit the stress-strain behavior of ductile polymeric materials. In all films formulations, it was observed that the elastic modulus followed the same trend as the TS. The main tensile

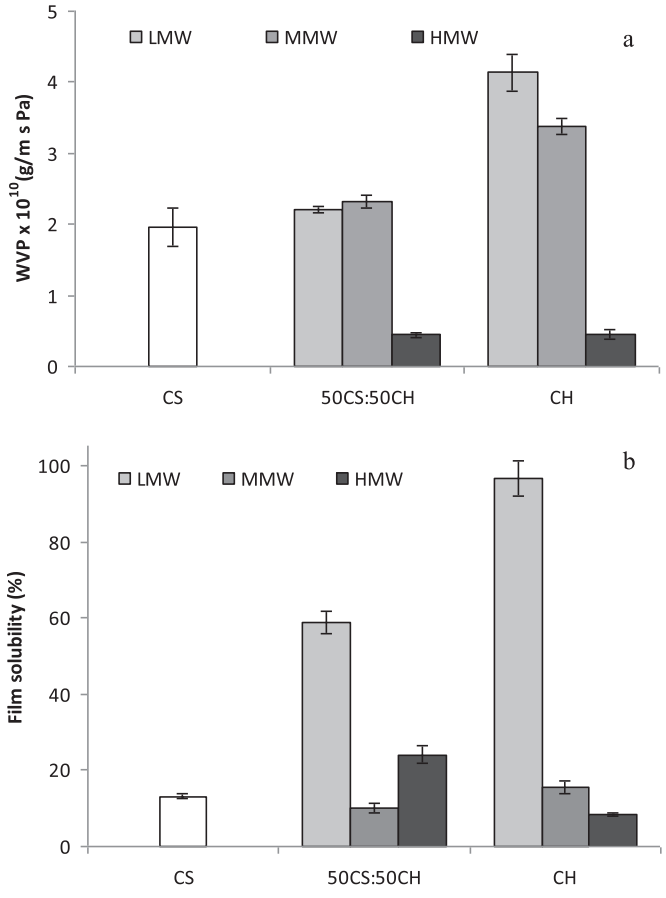

Fig. 3. a) Water vapor permeability and b) solubility of films based on corn starch (CS), chitosan (CH) and a blend of them in equal proportions. LMW, MMW and HMW correspond to low, medium and high molecular weight chitosan.

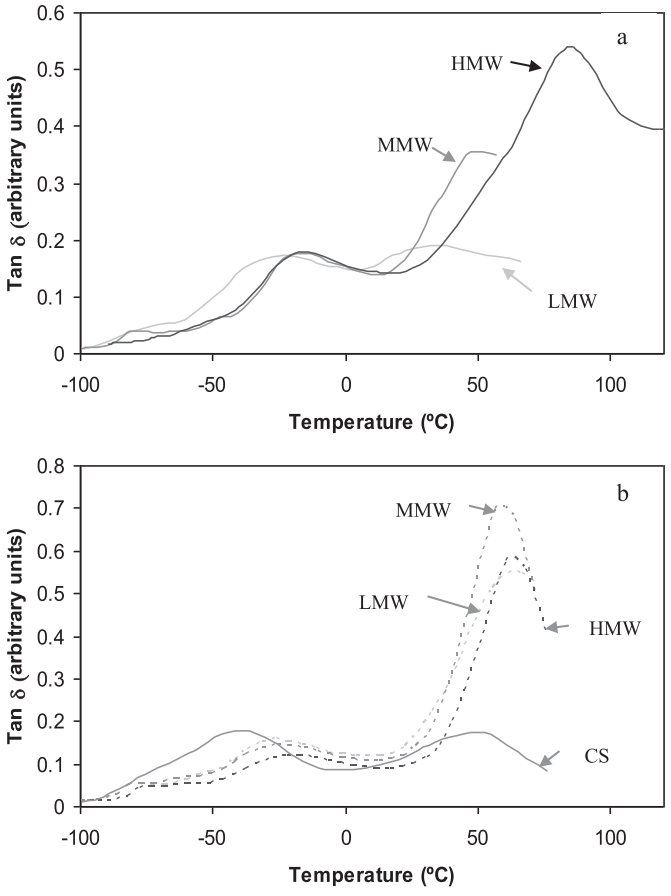

Fig. 4. DMA spectra (dependence of tan δ with temperature at a constant frequency of 20 Hz) of films based on corn starch (CS), chitosan (CH) and a blend of them in equal proportions. LMW, MMW and HMW correspond to low, medium and high molecular weight chitosan.

parameters of CS films were: TS = 8.94 ± 0.62 MPa, E = 30.7 ± 2.62 MPa and EB = 27.11 ± 2.04%. These values were within the range of those reported by other authors for plasticized starch-based films (Mali, Grossmann, García, Martino, & Zaritzky, 2002; López et al., 2008, 2011).

Mechanical profile of CH films depended strongly on its molecular weight, (Fig. 5). While films formulated with HMW chitosan were brittle and rigid, because they showed high elastic modulus and tensile strength values and low elongations at break, those derived from MMW and LMW ones result extremely deformable and flexible, (Fig. 5). This could be attributed to the effects of the chitosan molecular weight on the type and number of polymer–polymer, polymer–plasticizer and polymer–solvent interactions, which determine the polymer matrix structure and characteristics. HMW chitosan presents high polymerization degree chains, which favors polymer–polymer interactions, leading to strong matrices, typical of the high resistance films. Contrary, for LMW chitosan, polymer-plasticizer and polymer–solvent interactions became important and the development of high extensible materials is favored. A similar explanation was also argued by Martínez-Camacho et al. (2010) who also stressed that the presence of the plasticizer in the films made with medium molecular weight chitosan reduces the necessary effort for the deformation, as well as the deformation of the films before their rupture. Leceta et al. (2013) working on chitosan-based films reported that TS and elastic modulus increased while elongation at break decreased when chitosan molecular weight increased, due to the formation of more compact network.

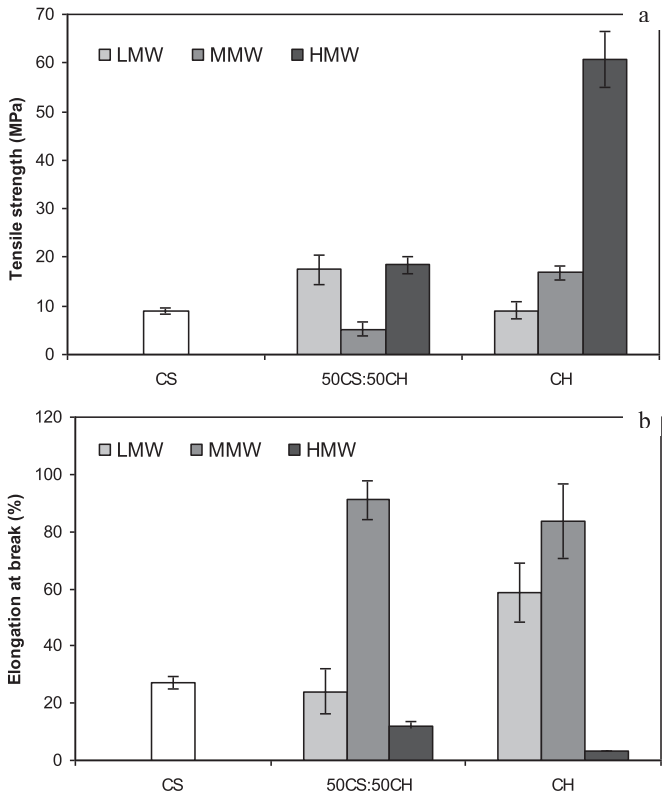

Fig. 5. Tensile mechanical properties of films based on corn starch (CS), chitosan (CH) and a blend of them in equal proportions. a) tensile strength and b) elongation at break. LMW, MMW and HMW correspond to low, medium and high molecular weight chitosan.

Likewise, there is a broad range of reported data in literature of mechanical properties of CH films; differences may be attributed to CH composition and suppliers, as well as film preparation techniques (Leceta et al., 2013; Park et al., 2002; Rivero, García, & Pinotti, 2012; Xu et al., 2005).

Tensile mechanical behavior of blend films was strongly affected by CH molecular weight. TS value of HMW-blend films was intermediate between one component ones, while those derived from MMW showed an antagonic effect and those of LMW registered a synergic one (Fig. 5a). Xu et al. (2005) stressed that linear amylose molecules can readily aligned closely or associate with similar linear chitosan molecules to form the intermolecular hydrogen bonds, the extension of this interaction is controlled by chitosan molecular weight, which helps to explain the described synergic or antagonic effect. Likewise, elongation at break values of LMW-blend films did not significantly ($p > 0.05$) differ from that of CS, although it was lower ($p < 0.05$) than the value of the corresponding CH film (Fig. 4b). In the case of MMW-blend the opposite behavior was observed, while for HMW-blends the obtained values were intermediate between individual CS and CH films.

Furthermore, the mechanical properties were evaluated by uniaxial tension tests through DMA. The stress–strain curves showed the mechanical responses of the LMW-CH based films (Fig. 6). In all cases, the model proposed used to estimate the elastic modulus fitted the experimental data satisfactorily ($r^2 > 0.93$); the obtained values for dynamical mechanical parameters are presented in the Table insert in Fig. 6. Under uniaxial tests, CS films are characterized by high E_c values, and low strain and stress, being the obtained values within the range of those reported for reinforced cassava starch films (Versino & García, 2014) and plasticized corn starch films (Muscat, Adhikari, Adhikari, & Chaudhary, 2012). Regarding to CH-based films, the significantly ($p < 0.05$) higher dynamic elastic modulus obtained for HMW-CH films was in agreement with the brittle and rigid tensile mechanical behavior previously described. The lower E_c values reported for MMW-CH and LMW-CH, as well as the higher strain registered, are again indicative of deformable and flexible materials, (Table insert in Fig. 6). These results reinforce the idea that polymer matrix structure development and film characteristics depend on chitosan molecular weight. Dynamic mechanical behavior of blend films was affected by CH molecular weight, while blend films containing MMW-CH show a similar behavior than CS films, LMW and HMW-CH films exhibited an antagonic effect (Fig. 6), which is contrary to that observed in tensile tests. Likewise, Salaberria, Diaz, Labidi, and Fernandes (2015) informed similar dynamic elastic modulus for thermoplastic starch films containing chitin nanocrystals and nanofibers.

Additionally, Table 3 showed the puncture mechanical parameters of formulated films. Although maximum force of CH films was higher than those of CS ones, no clear effect of molecular weight on the studied parameters is observed. In the case of blend films, LMW-CH films exhibited a maximum force closer to the corresponding CH one; meanwhile HMW-CH blends showed the highest value and MMW-CH blends the lowest. These results are in agreement with those obtained by tensile assays (TS) and uniaxial tension tests (E_c) previously reported. Values corresponding to MMW-CH based films attract attention and could be attributed to the high moisture content of the samples (Table 3). In general, the area under the curve, which is indicative of the energy required to puncture the films follows a similar trend than the maximum force. The higher deformation values of films containing LMW and MMW-CH are again indicative of deformable and flexible film matrices.

3.7. Microstructural analysis: SEM and FTIR

SEM was used to examine the microstructure and polymer compatibility of developed films. Plasticized corn starch films showed homogeneous surfaces and compact structures (Fig. 7a), which are in agreement with its relative lower water vapor permeability and high dynamic elastic modulus (Figs. 3 and 6). SEM micrographs of the cross-sections of plasticized chitosan films exhibited homogeneous structures, the higher the MW the more compact the structure. Fig. 7b shows the typical behavior for LMW-chitosan based materials, in this case the presence of pores helps to explain its poor water vapor barrier properties. Composite films show dense cross-sections which are indicative of high compatible polymers (Fig. 7c). Besides, the effect of film formulation on the thickness can be noticed.

FTIR technique helps us to analyze the functional groups of the polymeric films in order to determine the possible interactions between CH and CS in composite systems. Fig. 8 shows the IR spectra of CH films derived from different molecular weight polymers; in general, LMW-CH films exhibited a better definition of absorption peaks than MMW and HMW ones. The spectral window located in the region between 3600 and 3000 cm^{-1} experienced a broadening with increasing molecular weight of chitosan, which indicates a greater intensity of the hydrogen bonds between the polymer with both the plasticizer and water molecules associated to film structure (Fig. 8a). This broad band can be attributed to the characteristic absorption peak of amino groups in the region of 3400–3500 cm^{-1}, which is masked by the broad absorption band of the –OH group (López et al., 2014; Martínez-Camacho et al., 2010; Sionkowska, Wisniewski, Skopinska, Kennedy, & Wess, 2004). Likewise, peaks located in the region of 3000–2800 cm^{-1} were detected, which can be attributed to the symmetric and anti-symmetric stretching modes of C–H in methyl (CH_3) and methylene (CH_2) functional group (López et al., 2014).

Within the 2000–800 cm^{-1} spectral window (Fig. 8b), the typical absorption bands of the polymer are situated at 1656 and 1551 cm^{-1}, corresponding to amide I and amide II, respectively (Wu et al., 2005). Besides, peaks around 901 and 1155 cm^{-1}, and peak at

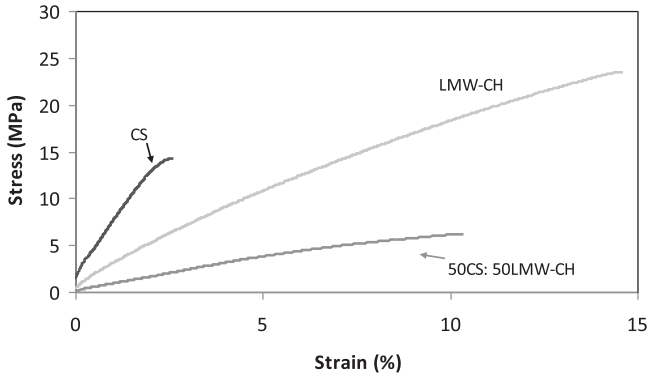

Dynamic mechanical parameters of plasticized films formulated with corn starch, different molecular weight chitosan and the blend of both in equal proportions.

Film formulation	*Chitosan molecular weight (MW)*	*Dynamic mechanical parameters by uniaxial tension tests*				
		Dynamic elastic modulus, E_c (MPa)	*K fitting parameter of eq. 9*	r^2	*Maximum strain (%)*	*Maximum stress (MPa)*
Corn starch (CS)*	-	1235 ± 362^{d}	41.6 ± 27.5^{c}	0.930	2.05 ± 0.79^{a}	11.91 ± 3.38^{b}
50 CS: 50 CH	LMW	105 ± 33^{a}	$5.3 \pm 2.1^{a,b}$	0.984	$9.04 \pm 1.42^{d,e}$	5.77 ± 0.62^{a}
	MWM	1385 ± 240^{d}	24.6 ± 2.3^{c}	0.982	4.67 ± 0.58^{b}	20.9 ± 3.52^{c}
	HMW	133 ± 19^{a}	$6.4 \pm 1.1^{a,b}$	0.999	9.09 ± 0.42^{d}	22.30 ± 2.21^{c}
Chitosan (CH)	LMW	338 ± 116^{b}	$5.2 \pm 2.7^{a,b}$	0.992	12.82 ± 2.5^{e}	22.88 ± 0.81^{c}
	MWM	400 ± 22^{b}	$4.8 \pm 0.8^{a,b}$	0.999	7.97 ± 0.21^{c}	21.18 ± 0.73^{c}
	HMW	656 ± 162^{c}	4.0 ± 0.2^{a}	0.999	7.69 ± 0.24^{c}	48.61 ± 2.62^{d}

*CS: 4% (w/w) corn starch gelatinized suspension, CH: 2.5% (w/w) CH solution and 50CS: 50CH: the blend of them in equal proportion (w/w). All formulations contain glycerol as plasticizer to 25% w/w solids. LMW: low molecular weight, MMW: medium molecular weight and HMW: high molecular weight chitosan. Reported values correspond to the mean ± standard deviation. Different letters in the same column indicate significant differences ($p < 0.05$).

Fig. 6. Stress–strain curves and dynamic mechanical parameters obtained by uniaxial tension tests of films based on corn starch (CS), chitosan (CH) and a blend of them in equal proportions. LMW, MMW and HMW correspond to low, medium and high molecular weight chitosan.

1591 cm^{-1}, which exhibited a better definition in LMW-CH films, were observed (Fig. 8b). These absorption peaks were assigned by Cheng et al. (2003) to saccharide structure and amino groups, respectively.

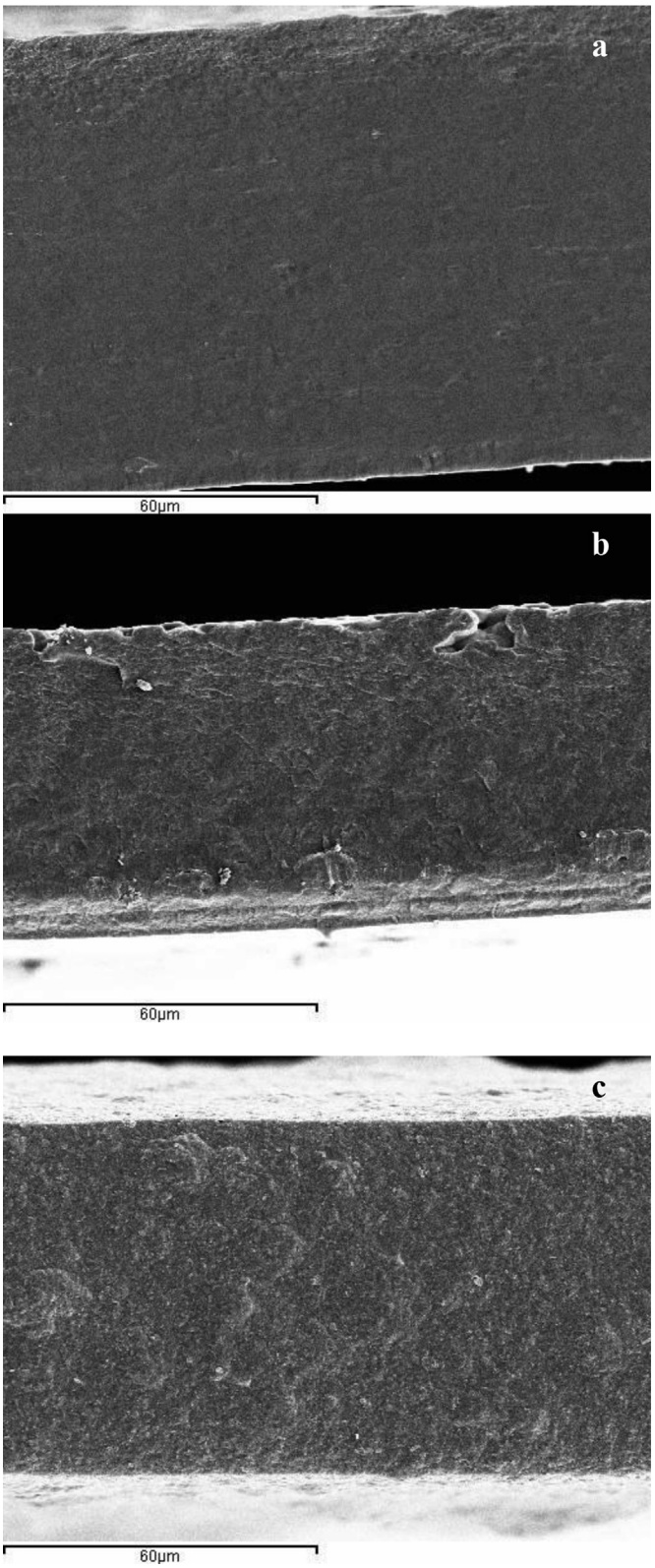

Fig. 7. SEM micrographs of cross-sections of films plasticized: a) corn starch, (b low molecular weight chitosan and c) the blend of them in equal proportions. Magnification used 1000×.

With regard to CS films (Fig. 9), peaks located at 920, 1074 and 1156 cm^{-1} were identified, which corresponds to C–O bond stretching, being that at 1074 cm^{-1} (less defined) characteristic of the anhydroglucose ring stretch (Zhang & Han, 2006). The peak observed at 1413 cm^{-1} is attributed to the symmetric deformation mode $-CH_3$ (Salleh, Muhamad, & Khairuddin, 2009). The bands appearing at 1459 (less defined) and 1661 cm^{-1} were assigned to the OH group of water δ bending and CH3 one, respectively (Mano, Koniarova, & Reis, 2003). These results are comparable with those reported by other authors (Fang, Fowler, Tomkinson, & Hill, 2002; Kacuráková & Wilson, 2001; López et al., 2014; Zhang & Han, 2006). The extremely broad band that appears with a maximum intensity at 3434 cm^{-1} corresponds to the hydrogen bonding interactions of hydroxyl groups. As was previously described, this band corresponds to the associated stretching vibrational complex with free hydroxyl groups and evidenced the formation of inter- and intramolecular hydrogen bonding in plasticized starch films (Fang et al., 2002; Wu, 2003).

FTIR spectra of blend films exhibited the typical signals of both starch and chitosan. As in the case of one component film spectra, the signal of LMW-CH films were better defined than MMW and HMW ones. The peak appearing at 2929 cm^{-1} is characteristic of the C–H bond stretching and can be observed in all spectra. The amplitude increase of 3400 cm^{-1} signal (Fig. 9a) is again indicative of the development of hydrogen bonding interactions in blend films, which is the predominant interaction mechanism between hydrophilic polymers.

Spectra of composite films presented small modifications in the position of some bands within the range of 1500–1700 cm^{-1} that are related to amino and carbonyl groups. Fig. 9b shows that in blends films, the absorption band located at 1661 cm^{-1} in the CS-based films, attributed to flexural vibrations of OH groups, is overlapped with the amide I around 1656 cm^{-1} in CH based ones which undergoes a shift to smaller wavenumbers in the case of blends, registering at 1652, 1650 and 1655 cm^{-1} for LMW, MMW and HMW respectively. The shifts observed as well as the decrease in the absorption signal indicate the development of interactions between CS and CH functional groups. These results evidence the compatibility of both polymers, being the interactions attributed to the similar chemical and geometrical linear structure of both starch and chitosan. Similar results were reported by Martínez-Camacho et al. (2010) working with commercial and shrimp waste silage extracted chitosans, who pointed out that the rightward shift of the amide I peak suggests that chitosan $-NH_2$ groups are compromised in hydrogen bonds formation.

Likewise, in CH based films the appearance of a shoulder at 1460-1457 cm^{-1}, was observed (Figs. 8b and 9b), and attributed to the stretching of the CH_2 group (Wilhelm, Sierakowski, Souza, & Wypych, 2003). This signal indicates that the plasticizer added was chemically bonded to the polymeric chains, demonstrating the internal plasticization of the CH matrix.

4. Conclusions

Chitosans used in this work were characterized and classified according to its molecular weight; the acetylation degree was similar for all tested products. Filmogenic solutions based on LMW-CH exhibited a Newtonian rheological behavior while those containing MMW or HMW-CH pseudoplastic one, increasing both consistency index and apparent viscosity with polymer molecular weight.

Chitosan based film physicochemical properties were strongly affected by its molecular weight: the lower the MW the higher the color differences (ΔE) and film solubility.

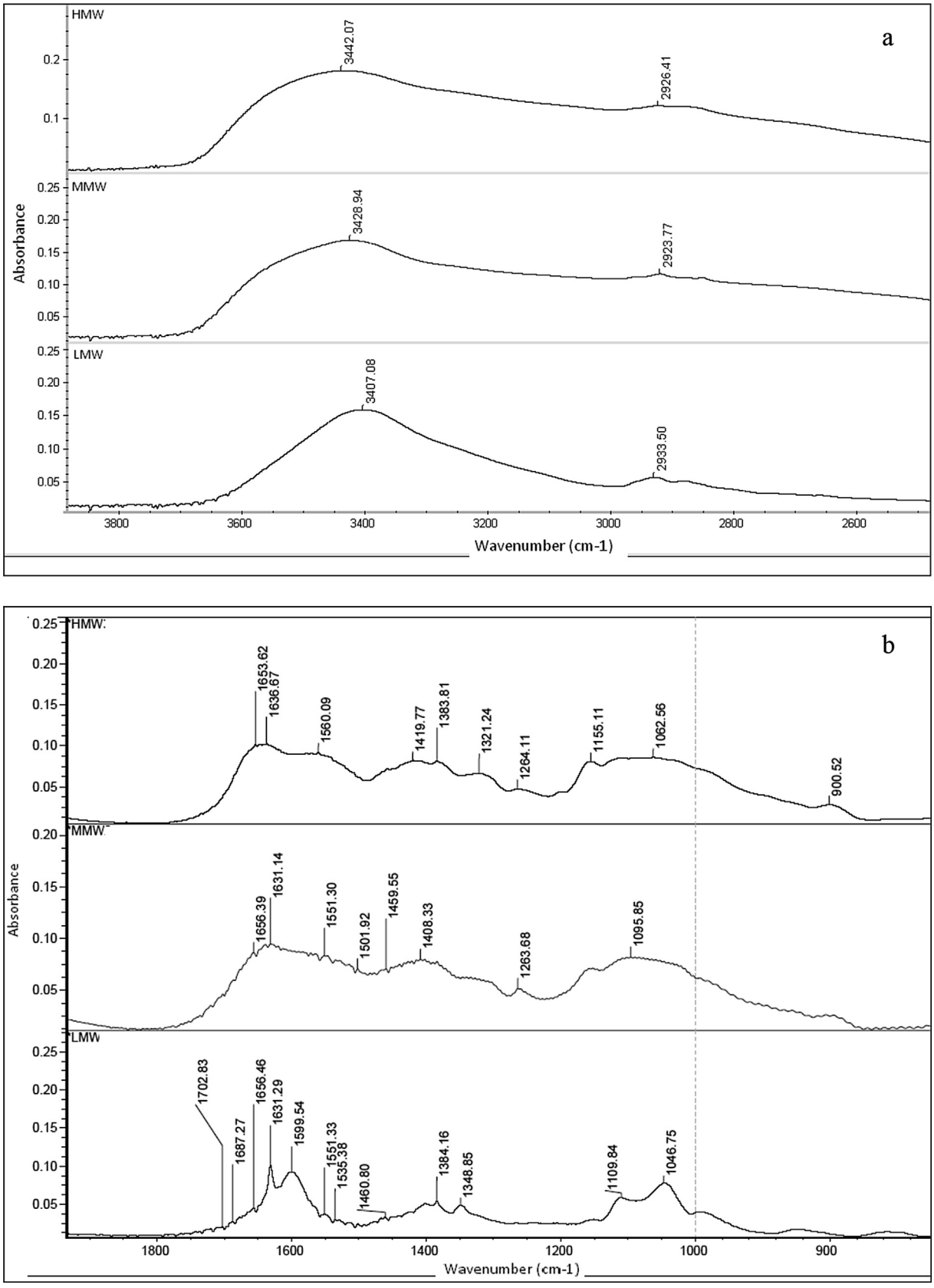

Fig. 8. Effect of chitosan molecular weight on FTIR spectra of chitosan based films: a) 4000–2500 cm^{-1} spectral window and b) 1900–800 cm^{-1} spectral window. LMW, MMW and HMW correspond to low, medium and high molecular weight chitosan.

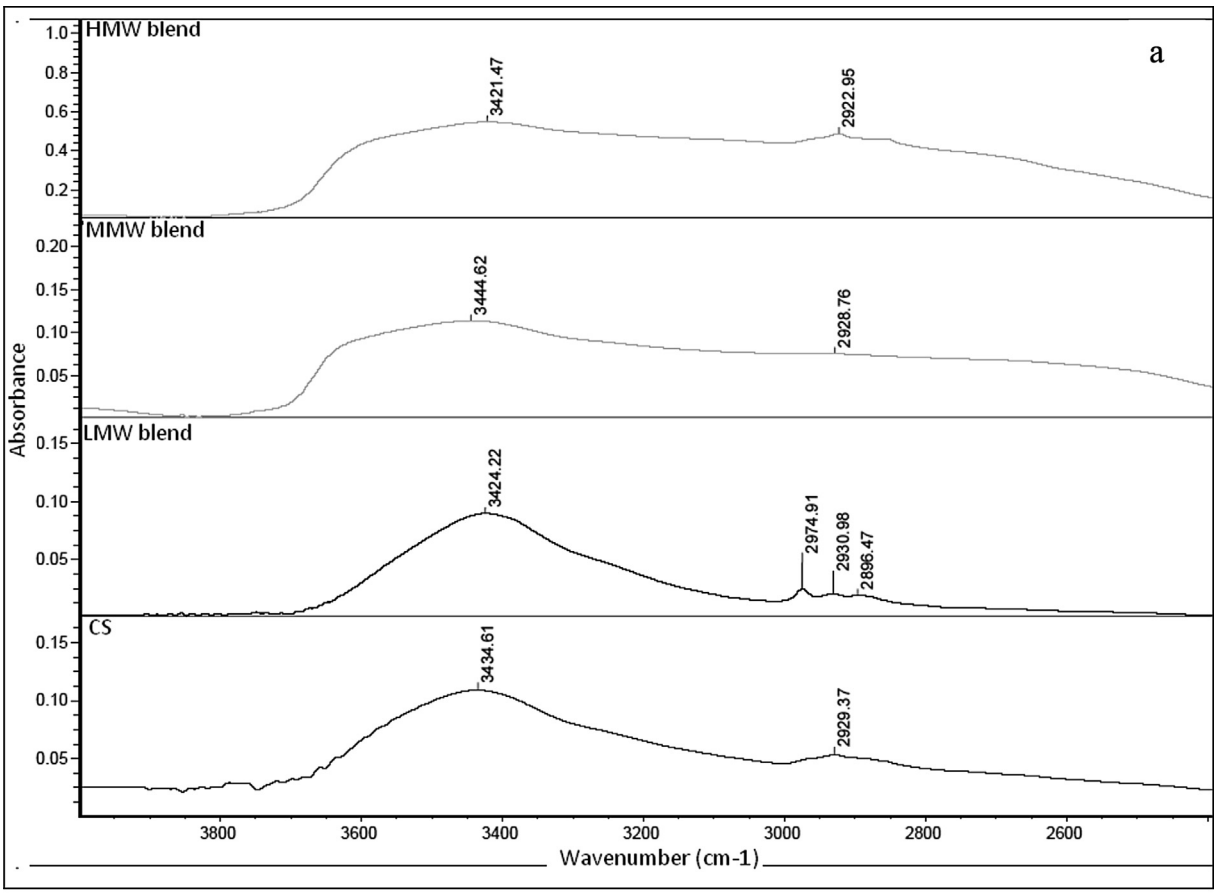

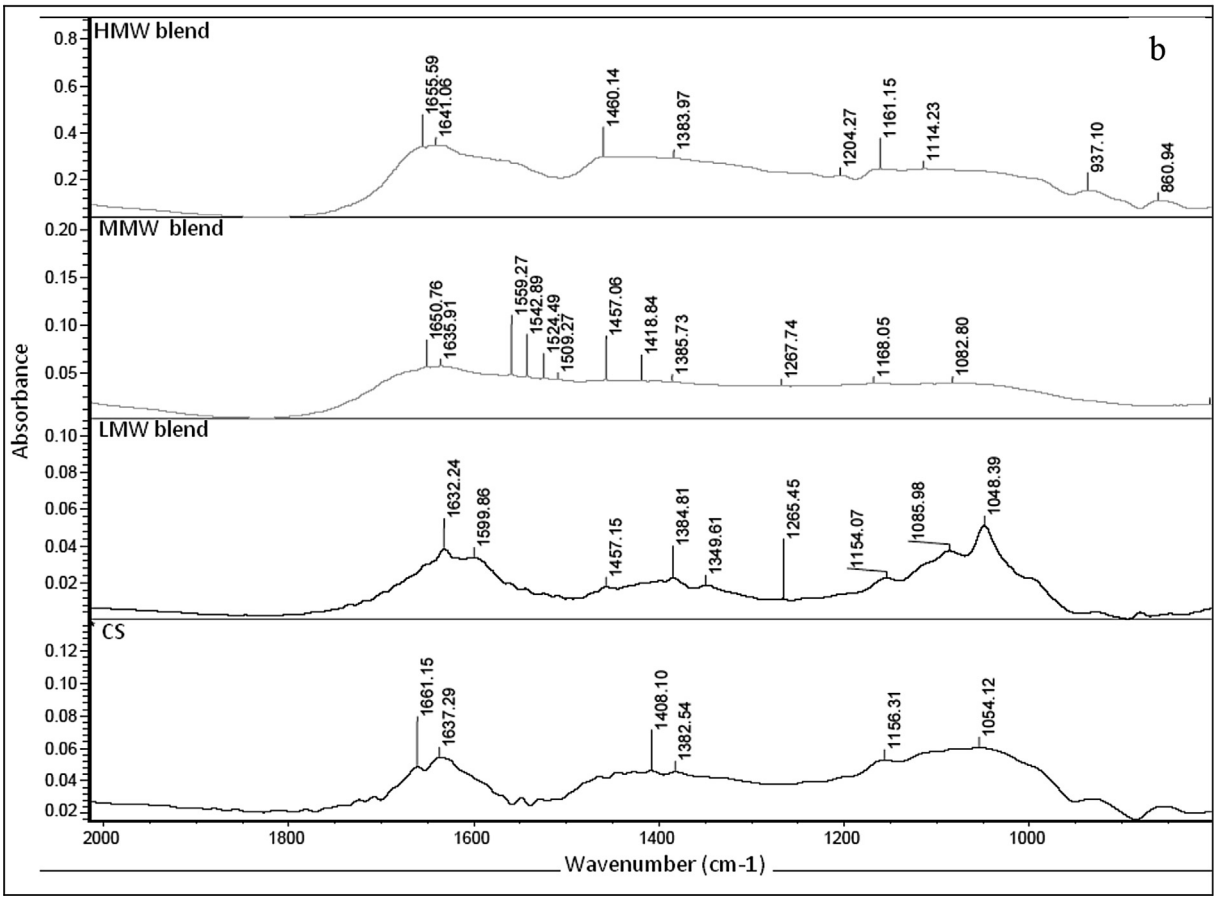

Fig. 9. Effect of chitosan molecular weight on FTIR spectra of blend films: a) 4000−2500 cm^{-1} spectral window and b) 1900−800 cm^{-1} spectral window. CS corresponds to corn starch; LMW, MMW and HMW correspond to low, medium and high molecular weight chitosan.

SEM observations demonstrated that plasticized chitosan films exhibited homogeneous structures, the higher the MW the more compact the structure and the lower the WVP. In this materials, the broadening of the band at 3600–3000 cm^{-1} of FTIR spectra with increasing molecular weight of chitosan, indicates a greater intensity of the hydrogen bonds between the polymer with both the plasticizer and water molecules associated to film structure.

Likewise, CH and CS were compatible polymers which led to the development of homogeneous blend films. The possible polymer interactions were evidenced by the shifts observed within the region of 1500–1700 cm^{-1} as well as the decrease in the absorption signal in FTIR spectra. These interactions, mainly hydrogen bonding type, reduce the hydrophilic groups' availability of chitosan matrices, leading to a reduction in water vapor transmission rate of composite films.

In this work, a comprehensive study of the mechanical properties of the developed films was performed through different complementary tests like tensile, uniaxial tension and puncture tests. Chitosan molecular weight affects both the type and number of polymer–polymer, polymer–plasticizer and polymer–solvent interactions, which determine the matrix structure and characteristics. In HMW chitosan matrix polymer–polymer interactions are favored, leading to strong and resistant matrices with high dynamic elastic modulus values and high Tg. In the case of LMW chitosan based ones, polymer-plasticizer and polymer–solvent interactions became important and the development of high extensible and soluble materials is privileged.

Therefore, an integral approach of molecular weight chitosan effect on film performance has been carried out; these results are relevant achievements in relation to the interrelation between film structure and its macroscopic final properties of biodegradable materials.

Acknowledgments

The financial support provided by UNER (Project PID-UNER 8066) and ANPCyT (Project PICT 2011 – 1213) of Argentina is gratefully acknowledged. Authors wish to thank to Eng. J. Lecot and D. Russo for his technical assistance on DMA assays as well as Dr. A. Jiménez for his assistance with SEM micrographs.

References

Arancibia, M. Y., López-Caballero, M. E., Gómez-Guillén, M. C., Fernández-García, M., Fernández-Martín, F., & Montero, P. (2015). Antimicrobial and rheological properties of chitosan as affected by extracting conditions and humidity exposure. *LWT – Food Science and Technology, 60*, 802–810.

ASTM Standard E96/E96M. (2012). *Standard test methods for water vapor transmission of material*. West Conshohocken, PA: ASTM International. http://www.astm.org.

Avérous, L., Fringant, C., & Moro, L. (2001). Plasticized starch-cellulose interactions in polysaccharide composites. *Polymer, 42*, 6565–6572.

Bangyekan, C., Aht-Ong, D., & Srikulkit, K. (2006). Preparation and properties evaluation of chitosan-coated cassava starch films. *Carbohydrate Polymers, 63*, 61–71.

Beaney, P., Lizardi-Mendoza, J., & Healy, M. (2005). Comparisons of chitins produced by chemical and bioprocessing methods. *Journal of Chemical Technology and Biotechnology, 80*, 145–150.

Bof, M. J., García, M. A., Locaso, D., & Zambón, Y. (2014). Películas compuestas a base de almidón y quitosano: formulación y caracterización. In *Proceedings of the International Conference on Food Innovation. FoodInnova 2014* (3rd ed.). (p. 148). Concepción del Uruguay: Universidad Nacional de Entre Ríos.

Casettari, L., Cespi, M., Palmieri, G. F., & Bonacucina, G. (2013). Characterization of the interaction between chitosan and inorganic sodium phosphates by means of rheological and optical microscopy studies. *Carbohydrate Polymers, 91*, 597–602.

Cheng, M., Deng, J., Yang, F., Gong, Y., Zhao, N., & Zhang, X. (2003). Study on physical properties and nerv cell affinity of composite films from Chitosan and gelatin solutions. *Biomaterials, 24*, 2871–2880.

Chen, J. L., & Zhao, Y. (2012). Effect of molecular weight, acid, and plasticizer on the physicochemical and antibacterial properties of β-chitosan based films. *Journal of Food Science, 77*(5), 127–136.

Chillo, S., Flores, S., Mastromatteo, M., Conte, A., Gerschenson, L., & Del Nobile, M. A. (2008). Influence of glycerol and chitosan on tapioca starch-based edible film properties. *Journal of Food Engineering, 88*, 159–168.

Da Roz, A. L., Carvalho, A. J. F., Gandini, A., & Curvelo, A. A. S. (2006). The effect of plasticizers on thermoplastic starch compositions obtained by melt processing. *Carbohydrate Polymers, 63*, 417.

Dutta, P. K., Tripathi, S., Mehrotra, G. K., & Dutta, J. (2009). Perspectives for chitosan based antimicrobial films in food applications. *Food Chemistry, 114*(4), 1173–1182.

Famá, L., Flores, S. K., Gerschenson, L., & Goyanes, S. (2006). Physical characterization of cassava starch biofilms with special reference to dynamic mechanical properties at low temperatures. *Carbohydrate Polymers, 66*, 8–15.

Fang, J. M., Fowler, P. A., Tomkinson, J., & Hill, C. A. (2002). The preparation and characterization of a series of chemically modified potato starches. *Carbohydrate Polymers, 47*, 245–252.

García, N. L., Famá, L., Dufresne, A., Aranguren, M., & Goyanes, S. (2009). A comparison between the physico-chemical properties of tuber and cereal starches. *Food Research International, 42*, 976–982.

Han, J. H., & Gennadios, A. (2005). Edible films and coatings: a review. In J. H. Han (Ed.), *Innovations in food packaging* (pp. 239–262). London: Academic Press.

Huggins, M. L. (1942). The viscosity of dilute solutions of long-chain molecules. IV. Dependence on concentration. *Journal of the American Chemical Society, 64*(11), 2716–2718.

Hwang, K. T., Kim, J. T., Jung, S. T., Cho, G. S., & Park, H. J. (2003). Properties of chitosan based biopolymer films with various degrees of deacetylation and molecular weights. *Journal of Applied Polymer Science, 89*(13), 3476–3484.

Kacuráková, M., & Wilson, R. H. (2001). Developments in mid-infrared FT-IR spectroscopy of selected carbohydrates. *Carbohydrate Polymers, 44*, 291–303.

Kramer, E. O. (1938). Molecular weight of celluloses and cellulose derivates. *Journal of Industrial and Engineering Chemistry, 30*, 1200–1203.

Leceta, I., Guerrero, P., & de la Caba, K. (2013). Functional properties of chitosan-based films. *Carbohydrate Polymers, 93*, 339–346.

López, O. V., García, M. A., Villar, M. A., Gentili, A., Rodriguez, M. S., & Albertengo, L. (2014). Thermo-compression of biodegradable thermoplastic corn starch films containing chitin and chitosan. *LWT – Food Science and Technology, 57*, 106–115.

López, O. V., García, M. A., & Zaritzky, N. E. (2008). Film forming capacity of chemically modified corn starches. *Carbohydrate Polymers, 73*, 573–581.

López, O. V., Lecot, C. J., Zaritzky, N. E., & García, M. A. (2011). Biodegradable packages development from starch based heat sealable films. *Journal of Food Engineering, 105*, 254–263.

Ma, X., Chang, P., Yu, J., & Stumborg, M. (2009). Properties of biodegradable citric acid-modified granular starch/thermoplastic pea starch composites. *Carbohydrate Polymers, 75*, 1–8.

Mali, S., Grossmann, M. V. E., García, M. A., Martino, M. N., & Zaritzky, N. E. (2002). Microstructural characterization of yam starch films. *Carbohydrate Polymers, 50*, 379–386.

Mancini, M., Moresi, M., & Rancini, R. (1999). Mechanical properties of alginate gels: empirical characterisation. *Journal of Food Engineering, 39*, 369–378.

Mano, J. F., Koniarova, D., & Reis, R. L. (2003). Thermal properties of thermoplastic starch/synthetic polymer blends with potential biomedical applicability. *Journal of Materials Science: Materials in Medicine, 14*, 127–135.

Martínez-Camacho, A. P., Cortez-Rocha, M. O., Ezquerra-Brauer, J. M., Graciano-Verdugo, A. Z., Rodriguez-Félix, F., Castillo-Ortega, M. M., et al. (2010). Chitosan composite films: thermal, structural, mechanical and antifungal properties. *Carbohydrate Polymers, 82*, 305–315.

Mathew, S., & Abraham, T. E. (2008). Characterisation of ferulic acid incorporated starch–chitosan blend films. *Food Hydrocolloids, 22*(5), 826–835.

Mathew, S., Brahmakumar, M., & Abraham, T. E. (2006). Microstructural imaging and characterization of the mechanical, chemical, thermal, and swelling properties of starch–chitosan blend films. *Biopolymers, 82*(2), 176–187.

Mathew, A. P., & Dufresne, A. (2002). Morphological investigation of nanocomposites from sorbitol plasticized starch and tunicin whiskers. *Biomacromolecules, 3*, 609–617.

Motta de Moura, C., Motta de Moura, J., Madeira Soares, N., & de Almeida Pinto, L. A. (2011). Evaluation of molar weight and deacetylation degree of chitosan during chitin deacetylation reaction: used to produce biofilm. *Chemical Engineering and Processing, 50*, 351–355.

Mucha, M., & Pawlak, A. (2005). Thermal analysis of chitosan and its blends. *Thermochimica Acta, 427*(1–2), 69–76.

Muscat, D., Adhikari, B., Adhikari, R., & Chaudhary, D. S. (2012). Comparative study of film forming behaviour of low and high amylase starches using glycerol and xylitol as plasticizers. *Journal of Food Engineering, 109*, 189–201.

Neto, C. G. T., Giacometti, J. A., Job, A. E., Ferreira, F. C., Fonseca, J. L. C., & Pereira, M. R. (2005). Thermal analysis of chitosan based networks. *Carbohydrate Polymers, 62*, 97–103.

Park, S. Y., Marsh, K. S., & Rhim, J. W. (2002). Characteristics of different molecular weight chitosan films affected by the type of organic solvents. *Journal of Food Science, 67*(1), 194–197.

Pelissari, F. M., Grossmann, M. V. E., Yamashita, F., & Pineda, E. A. G. (2009). Antimicrobial, mechanical, and barrier properties of Cassava Starch–Chitosan films incorporated with Oregano essential oil. *Journal of Agricultural and Food Chemistry, 57*(16), 7499–7504.

Pillai, C. K. S., Paul, W., & Sharma, C. P. (2009). Chitin and chitosan polymers: chemistry, solubility and fiber formation. *Progress in Polymer Science, 34*, 641–678.

Ravi Kumar, M. N. V. (2000). A review of chitin and chitosan applications. *Reactive and Functional Polymers, 46*(1), 1–27.
Rinaudo, M. (2006). Chitin and chitosan: properties and applications. *Progress in Polymer Science, 31*, 603–632.
Rivero, S., García, M. A., & Pinotti, A. (2012). Heat treatment to modify the structural and physical properties of chitosan-based films. *Journal of Agricultural and Food Chemistry, 60*(1), 492–499.
Roberts, G. A. F., & Domszy, J. G. (1982). Determination of the viscosimetric constants for chitosan. *International Journal of Biological Macromolecules, 4*, 374–377.
Salaberria, A. M., Diaz, R. H., Labidi, J., & Fernandes, S. C. M. (2015). Role of chitin nanocrystals and nanofibers on physical, mechanical and functional properties in thermoplastic starch films. *Food Hydrocolloids, 46*, 93–102.
Salleh, E., Muhamad, I., & Khairuddin, N. (2009). Structural characterization and physical properties of antimicrobial (AM) starch-based films. *World Academy of Science, Engineering and Technology, 31*, 428–436.
Sánchez-González, L., Cháfer, M., Chiralt, A., & González-Martínez, C. (2010). Physical properties of edible chitosan films containing bergamot essential oil and their inhibitory action on *Penicillium italicum*. *Carbohydrate Polymers, 82*(2), 277–283.
Sini, T. K., Santhosh, S., & Mathew, P. T. (2007). Study of the production of chitin and chitosan from shrimp shell by Bacillus subtilis fermentation. *Carbohydrate Research, 342*, 2423–2429.
Sionkowska, A., Wisniewski, M., Skopinska, J., Kennedy, C. J., & Wess, T. J. (2004). Molecular interactions in collagen and chitosan blends. *Biomaterials, 5*, 795–801.
Van den Broek, L. A. M., Knoop, R. J. I., Kappen, F. H. J., & Boeriu, C. G. (2015). Chitosan films and blends for packaging material. *Carbohydrate Polymers, 116*, 237–242.
Versino, F., & García, M. A. (2014). Cassava (*Manihot esculenta*) starch films reinforced with natural fibrous filler. *Industrial Crops and Products, 58*, 305–314.
Wilhelm, H., Sierakowski, M., Souza, G., & Wypych, F. (2003). Starch films reinforced with mineral clay. *Carbohydrate Polymers, 52*, 101–110.
Wu, C. (2003). Physical properties and biodegradability of maleated-polycaprolactone/starch composite. *Polymer Degradation and Stability, 80*, 127–134.
Wu, Y., Zheng, Y., Yang, W., Wang, C., Hu, J., & Fu, S. (2005). Synthesis and characterization of a novel amphiphilic chitosan–polylactide graft copolymer. *Carbohydrate Polymers, 59*, 165–171.
Xu, Y. X., Kim, K. M., Hanna, M. A., & Nag, D. (2005). Chitosan-starch composite film: preparation and characterization. *Industrial Crops and Products, 21*, 185–192.
Wu, Q. X., & Zhang, L. N. (2001). Properties and structure of soy protein isolate-ethylene glycol sheets obtained by compression molding. *Industrial and Engineering Chemistry, 40*, 1879–1883.
Younes, I., Sellimi, S., Marguerite Rinaudo, M., Jellouli, K., & Nasri, M. (2014). Influence of acetylation degree and molecular weight of homogeneous chitosans on antibacterial and antifungal activities. *International Journal of Food Microbiology, 185*, 57–63.
Zhang, Y., & Han, J. (2006). Mechanical and thermal characteristics of pea starch films plasticized with monosaccharides and polyols. *Journal of Food Science, 71*, 109–111.